J Physiol (2003), **550.3**, *pp.* 785–800

DOI: 10.1113/jphysiol.2003.042572
www.jphysiol.org

Journal of Physiology

GABA depolarizes neuronal progenitors of the postnatal subventricular zone via $GABA_A$ receptor activation

D. D. Wang *, D. D. Krueger † and A. Bordey *†

**Department of Neurosurgery and Cellular and Molecular Physiology and †Interdepartmental Neuroscience Graduate Program, Yale University School of Medicine, New Haven, CT 06520-8082, USA*

Previous studies have reported the presence of migrating and dividing neuronal progenitors in the subventricular zone (SVZ) and rostral migratory stream (RMS) of the postnatal mammalian brain. Although the behaviour of these progenitors is thought to be influenced by local signals, the nature and mode of action of the local signals are largely unknown. One of the signalling molecules known to affect the behaviour of embryonic neurons is the neurotransmitter GABA. In order to determine whether GABA affects neuronal progenitors via the activation of specific receptors, we performed cell-attached, whole-cell and gramicidin perforated patch-clamp recordings of progenitors in postnatal mouse brain slices containing either the SVZ or the RMS. Recorded cells displayed a morphology typical of migrating neuronal progenitors had depolarized zero-current resting potentials, and lacked action potentials. A subset of progenitors contained GABA and stained positive for glutamic acid decarboxylase 67 (GAD-67) as shown by immunohistochemistry. In addition, every neuronal progenitor responded to GABA via picrotoxin-sensitive $GABA_A$ receptor ($GABA_AR$) activation. $GABA_A$Rs displayed an ATP-dependent rundown and a low sensitivity to Zn^{2+}. GABA responses were sensitive to benzodiazepine agonists, an inverse agonist, as well as a barbiturate agonist. While GABA was hyperpolarizing at the zero-current resting potentials, it was depolarizing at the cell resting potentials estimated from the reversal potential of K^+ currents through a cell-attached patch. Thus, our study demonstrates that neuronal progenitors of the SVZ/RMS contain GABA and are depolarized by GABA, which may constitute the basis for a paracrine signal among neuronal progenitors to dynamically regulate their proliferation and/or migration.

(Resubmitted 5 March 2003; accepted after revision 7 May 2003; first published online 13 June 2003)
Corresponding author A. Bordey: Department of Neurosurgery, Yale University, 333 Cedar Street, LSOG 228, New Haven, CT 06520-8082, USA. Email: angelique.bordey@yale.edu

The subventricular zone (SVZ) has been identified as one of the largest germinal centres that persist in the adult mammalian brain (Levison & Goldman, 1997; Alvarez-Buylla & Temple, 1998; Garcia-Verdugo *et al.* 1998; Shihabuddin *et al.* 1999; Momma *et al.* 2000). Recently, there has been increasing evidence supporting the premise that in postnatal animals the anterior SVZ is a predominant source of neuronal progenitors; this holds important therapeutic promise (Zigova *et al.* 1998; Garcia-Verdugo *et al.* 1998; Luskin, 1998). Neuronal progenitors of the SVZ migrate along the rostro-caudal axis to the olfactory bulb via the rostral migratory stream (RMS) (Luskin, 1993; Lois *et al.* 1996), during which they also retain their ability to undergo mitosis. They also progressively differentiate during migration along the RMS (Baker *et al.* 2001; Coskun & Luskin, 2002). It is thought that the distinct steps of neurogenesis (i.e. migration, proliferation and differentiation) are influenced by interactions with the progenitor environment, including local cues within the SVZ/RMS and surrounding immature cells (Temple & Alvarez-Buylla, 1999). Thus, an understanding of the development of neuronal progenitors in the SVZ/RMS requires an analysis of the signals that influence neuronal progenitors in the SVZ and RMS.

Candidate molecules that may signal to neuronal progenitors include growth factors and neurotransmitters. Of particular interest is γ-aminobutyric acid (GABA), which has been shown to influence the proliferation (LoTurco *et al.* 1995; Antonopoulos *et al.* 1997; Haydar *et al.* 2000) and migration (Behar *et al.* 1996, 1998, 2000; Fueshko *et al.* 1998) of embryonic neuronal progenitors (Barker *et al.* 1998). Furthermore, functional $GABA_A$ receptors ($GABA_A$Rs) have been recently reported in postnatal neuronal progenitors cultured from the anterior SVZ (Stewart *et al.* 2002), suggesting a possible modulatory function of GABA on SVZ/RMS neuronal progenitors. However, it remains unclear whether GABA is present in postnatal progenitors of the SVZ/RMS. It also remains unclear whether functional $GABA_A$Rs are expressed in these cells in their near-intact environment as

previously shown for embryonic neuronal progenitors (LoTurco *et al.* 1995), as opposed to an artificial culture environment used to study postnatal neuronal progenitors (Stewart *et al.* 2002).

The role of GABA in embryonic cell migration and proliferation has been shown to be dependent on its effect on cell membrane potential, in particular its depolarizing action via $GABA_AR$ activation (LoTurco *et al.* 1995). It was also recently reported that as expected from studies on embryonic and immature neonatal neurons *in vitro* and in tissue slices (Mueller *et al.* 1983; LoTurco *et al.* 1995; Owens *et al.* 1996; Leinekugel *et al.* 1999), GABA depolarizes SVZ neuronal progenitors cultured from the SVZ (Stewart *et al.* 2002). However, it remains unclear whether GABA exerts a similar effect on the membrane potential of postnatal neuronal progenitors in their near-intact physiological environment.

Thus, to determine how GABA may influence neuronal progenitors in the SVZ/RMS, we performed cell-attached, whole-cell and gramicidin perforated patch-clamp recordings in corticostriatal slices of postnatal mice. $GABA_AR$s are primarily permeable to Cl^- (Bormann *et al.* 1987), and therefore using gramicidin will allow recordings that leave the intracellular [Cl^-] undisturbed (Myers & Haydon, 1972; Kyrozis & Reichling, 1995). We found that SVZ/RMS neuronal progenitors contain GABA and express functional $GABA_AR$s. Most significantly, we found that GABA depolarizes postnatal neuronal progenitors of the SVZ/RMS as previously reported for neonatal neurons (Luhmann & Prince, 1991; Leinekugel *et al.* 1999), as well as embryonic (LoTurco *et al.* 1995; Owens *et al.* 1996) and cultured SVZ (Stewart *et al.* 2002) neuronal progenitors. However, the reversal potential of GABA responses was more hyperpolarized than that in cultured SVZ progenitors (Stewart *et al.* 2002), yielding a lower intracellular [Cl^-] of 29 mM.

METHODS

Slice preparation

Corticostriatal slices including either the SVZ or the RMS were prepared as previously described for hippocampal and cortical slices (Bordey & Sontheimer, 1997, 2000; Bordey *et al.* 2001). These procedures were performed in accordance with the Institutional Animal Care and Use Committee, which is guided by US Government Principles for the Utilization and Care of Vertebrate Animals used in Testing, Research and Training. Briefly, 13- to 24-day-old CD-1 mice were anaesthetized using pentobarbital (50 mg kg^{-1}) and decapitated. The brain was quickly removed and chilled (0–4 °C) in 95 % O_2–5 % CO_2-saturated artificial cerebrospinal fluid (ACSF) containing (mM): NaCl 125; KCl 2.5; $CaCl_2$ 2; $MgCl_2$ 2; $NaHCO_3$ 25; glucose 10. For half of the experiments, slices were prepared in sucrose-based ASCF in which NaCl was replaced by 220 mM sucrose. The tissue of interest was glued to the stage of a vibratome and 250-μm-thick slices were cut in cold oxygenated ACSF. After a recovery period of > 1 h in ACSF, slices were placed in a flow-through chamber, held in position by a nylon mesh glued to a U-shaped platinum wire and continuously superfused with oxygenated ACSF at room temperature. The chamber was mounted on the stage of an upright microscope (Olympus BX50WI) equipped with a 60 × water immersion objective and infra-red optics.

Whole-cell recordings and cell identification

Whole-cell patch-clamp recordings were obtained as previously described (Edwards & Konnerth, 1992). Patch pipettes were pulled from thin-walled borosilicate glass (o.d., 1.55 mm; i.d., 1.2 mm; WPI, TW150F-40) on a PP-83 puller (Narishige, Japan). Pipettes had resistances of 6–8 MΩ when filled with one of the following solutions (mM): (1) KCl 140; $CaCl_2$ 1.0; $MgCl_2$ 2.0; ethylene glycol-bis(-aminoethyl ether)-*N*,*N*,*N*′,*N*′-tetraacetic acid (EGTA) 10; Hepes 10; pH adjusted to 7.2 with Tris-base; (2) solution 1 with addition of 4 mM MgATP or Na_2ATP plus 0.4 mM MgGTP; (3) solution 1 with addition of an ATP regenerating solution (Forscher & Oxford, 1985; MacDonald *et al.* 1989) that included 4 mM K_2ATP 4, 20 mM K_2-phosphocreatine, 50 U ml^{-1} creatine phosphokinase and 6 mM $MgCl_2$; KCl was reduced to 110 mM. The osmolarities of the intracellular and extracellular solutions were 295–300 and 305–310 mosmol l^{-1}, respectively. For morphological identification, 0.1 % Lucifer Yellow (LY, dilithium salt) was added to the pipette solution. Whole-cell recordings were performed using an Axopatch-200B amplifier (Axon Instruments). Current signals were low-pass filtered at 2–5 kHz and digitized on-line at 5–20 kHz using a Digidata 1320 digitizing board (Axon Instruments) interfaced with an IBM-compatible computer system. Data acquisition, storage and analysis were performed using pCLAMP version 8.0.2 (Axon Instruments). No correction of junction potentials was performed except for the perforated patch-clamp recordings. Whole-cell parameters (capacitance (C_M) and series resistance) were determined by compensating the transients of a small (5 mV) 10 ms hyperpolarizing voltage step. The capacitance reading of the amplifier was used as the value for C_M. C_M, the cell zero-current resting potential (V_R) and and the input resistance (R_M) were determined in the first 3 min of whole-cell recording. Voltage-clamp data in this study were limited to cells with an input resistance greater than 500 MΩ (determined at −70 mV). Images of cells visually chosen for recordings and LY fills were taken on-line and archived using LG3 frame grabber (Scion Corporation, MD, USA).

Data analysis

Peak currents were determined using Clampfit (Axon Instruments), and statistical values were evaluated with a statistical graphing and curve-fitting program (Origin, MicroCal). Statistical comparison of means was performed with Student's *t* test or ANOVA (Statview, SAS Institute Inc.). Data are represented as means ± S.D. in the text and as means ± S.E.M. on the graphs. The effects of picrotoxin and Zn^{2+} were expressed as I/I_{max}, the ratio of the GABA-induced peak current in the presence of the drugs divided by the control peak current amplitude. The dose–response and dose–inhibition curves were fitted with a logistic sigmoidal equation:

$$I/I_{max} = (I_1 - I_2)/[1 + ([GABA]/[GABA]_{½})^p] + 1,$$

where p is a constant related to the slope of the sigmoidal curve.

Perforated patch-clamp recordings

The cation-selective ionophore gramicidin was used for perforated-patch recordings to prevent interference with the intracellular Cl^- concentration ($[Cl^-]_i$) (Myers & Haydon, 1972; Kyrozis & Reichling, 1995). The gramicidin-containing pipette

solution was prepared fresh for each experiment from a stock solution (5 mg ml^{-1} in DMSO, stored at −20 °C) diluted in prefiltered intracellular solution (solution 1) to yield a final concentration of 5 μg ml^{-1}. To ensure full efficacy of the gramicidin, the solution was protected from light and renewed every 2 h. The liquid junction potential (4.4 mV) was corrected. Patch pipettes had a resistance of 5–6 MΩ when filled with the intracellular solution. Two precautions were used to minimize gramicidin ejection from the patch pipette when approaching the cells: positive pressure was avoided as much as possible and the pipette tip was filled with the normal intracellular solution by 10–15 s dipping (the gramicidin-containing solution was added by regular filling). Stable perforated recordings ($\leqslant$ 10 MΩ series resistances) were obtained in 12–15 min (Fig. 8*A* and *B*).

Using the reversal potential of K^+ currents through cell-attached patches to monitor the cell membrane potential, V_m

The method used to measure V_m from cell-attached K^+ currents is identical to that described by Verheugen *et al.* (1995, 1999) and Fricker *et al.* (1999). With a 158 mM K^+ pipette solution, which is close to the estimated intracellular [K^+] in other cell types (155 mM, Hille, 1992), the equilibrium potential for K^+ (E_K) across the patch is ~0 mV, and K^+ currents will reverse when the pipette potential (V_{pip}) cancels V_m out. Therefore, the cell holding potential ($-V_{pip}$) at which the K^+ current reverses direction gives a direct quantitative measure for V_m (at K^+ channel reversal, $V_{patch} = V_m - V_{pip} = E_K \approx 0$ mV). Depolarizing voltage ramps (Fig. 9) were applied to activate voltage-gated K^+ channels. For analysis of currents evoked by ramp stimulation, a correction was made for a leak component by linear fit and extrapolation of the closed level.

Drug applications

Both rapid bath and pressure applications were used. GABA was pressure applied by a computer-controlled pressure ejection system. Picrotoxin and $GABA_A$R modulators were applied by a rapid bath application system composed of a 6-channel-mini-valve perfusion system (Warner Instruments Corp., New Haven, CT, USA). Drugs were diluted in ACSF in which Hepes replaced $NaHCO_3$ and the pH was adjusted to 7.4 by NaOH.

GABA and GAD-65/67 immunostainings

After recordings, slices were fixed overnight in 4 % paraformaldehyde in phosphate-buffered saline containing 4 % sucrose (PBSS). Slices were washed three times in PBSS over 1 h, permeabilized for 20 min with 0.1 % Triton X-100, rinsed three times with PBSS, and then blocked overnight at 4 °C in PBSS containing 1 % bovine serum albumin (Sigma) and 10 % goat serum. Slices were incubated overnight (24 h) at 4 °C with primary antibody against GABA (1:500, Sigma, rabbit, catalogue number A2052) and with various primary antibodies against GAD-65 (Chemicon, mouse, MAB351R), GAD-65/67 (1:500, Stressgene, mouse, catalogue number MSA-225 and 1:500, rabbit, Sigma, catalogue number G5163) in blocking solution. Slices were subsequently washed three times with PBSS and incubated for 90 min at room temperature with various secondary antibody combinations: (1) goat anti-rabbit IgG conjugated to Cy2 (1:400, Jackson Labs) for GABA staining alone, (2) donkey anti-rabbit IgG conjugated to Alexa fluor 488 for GABA and goat anti-mouse IgG1 conjugated to Alexa fluor 568 for GAD (Stressgene) co-staining or goat anti-mouse IgG2 conjugated to Alexa fluor 568 for GAD-65 co-staining, (3) goat anti-mouse IgG1 conjugated to Alexa fluor 568 for GAD (Stressgene) and donkey anti-rabbit IgG conjugated to Alexa fluor 488 for GAD-65/67 (Sigma). All the Alexa Fluor secondary antibodies were bought from Molecular Probes and used at 1:1000. Finally, after three washes in PBSS, slices were mounted on glass coverslips with fluorescent mounting medium (Vectashield-DAPI, Vector) and were finally viewed on an epifluorescence microscope (Olympus microscope BX51) using standard procedures. For control experiments, we performed staining with only one of the primary antibodies and the two secondary antibodies normally used for the co-staining. When the primary antibody was not included, we did not observe any staining with the secondary antibody alone. Similarly, when one of the primary antibodies was not included but both secondary antibodies were present, we did not observe staining for the missing primary antibody. In addition, we tested the effect of using various concentrations of Triton X-100 (0, 0.1 and 0.3 %) in the blocking solution. We did not observe any significant difference in the degree of GAD and GABA staining in the SVZ/RMS performed with Triton X-100. However, GAD staining in the striatum appeared brighter with 0.1 % or 0.3 % Triton X-100 as compared to that obtained with no Triton X-100.

Chemicals were purchased from Sigma (Saint Louis, MO, USA) except K_2-phosphocreatine, which was purchased from Calbiochem (USA).

RESULTS

Whole-cell recordings were obtained from 157 visually identified cells located in corticostriatal slices from postnatal mice.

Identification of recorded cells as neuronal progenitors

Cell location and morphology. Previous studies have shown that a selected population of neuronal progenitors from the SVZ migrate and populate the RMS, a region that is mainly composed of neuronal progenitors (Luskin, 1993; Lois *et al.* 1996; Luskin, 1998; Gritti *et al.* 2002). Thus, we prepared coronal slices including either the SVZ or the RMS. Figure 1*A* shows a photograph of a caudal slice containing the SVZ, which lines the lateral ventricle. Figure 1*B* displays a rostral section containing the RMS distinguishable by its round shape and lighter appearance. At higher magnification, cells in the RMS were densely packed, forming a channel of cells that protrude from the surrounding tissue (inset in Fig. 1*B*). The SVZ consisted of a 30- to 40-μm-wide band of cells, separated from the ventricle by ependymal cells displaying characteristic cilia (data not shown). To identify the morphology of the recorded cells, cells were filled with Lucifer Yellow (LY) and visualized during the recording. Photographs of typical cells recorded in the SVZ or RMS are shown in Fig. 1*C*. Most of the cells recorded in the SVZ and RMS had small, round cell bodies (diameter of 6–8 μm) with one or two short, bipolar processes. The processes had various lengths and shapes as illustrated in Fig. 1*C*. Such diversity in the length and shape of processes is expected for migrating cells, including SVZ and RMS progenitors (Kakita & Goldman, 1999; Murase & Horwitz, 2002). These cells closely resemble migrating neuronal progenitors described *in vivo* (Doetsch *et al.* 1999) and *in vitro* (Wichterle *et al.* 1997; Stewart *et al.* 1999).

Passive membrane properties of SVZ and RMS cells. When combining the data from both regions, cells had a mean zero-current resting membrane potential (measured as the mean zero current level) (V_R) of −21.9 ± 9.3 mV (mean ± S.D., $n = 150$), an input resistance (R_M) of 3.7 ± 1.9 GΩ ($n = 150$) and a whole-cell membrane capacitance (C_M) of 6.6 ± 2.5 pF ($n = 150$). In order to confirm the identification of the recorded cells as neuronal progenitors, we determined and compared the electrophysiological properties of cells in the RMS and SVZ to those published for neuronal progenitors cultured from the SVZ. Both SVZ and RMS cells showed similar

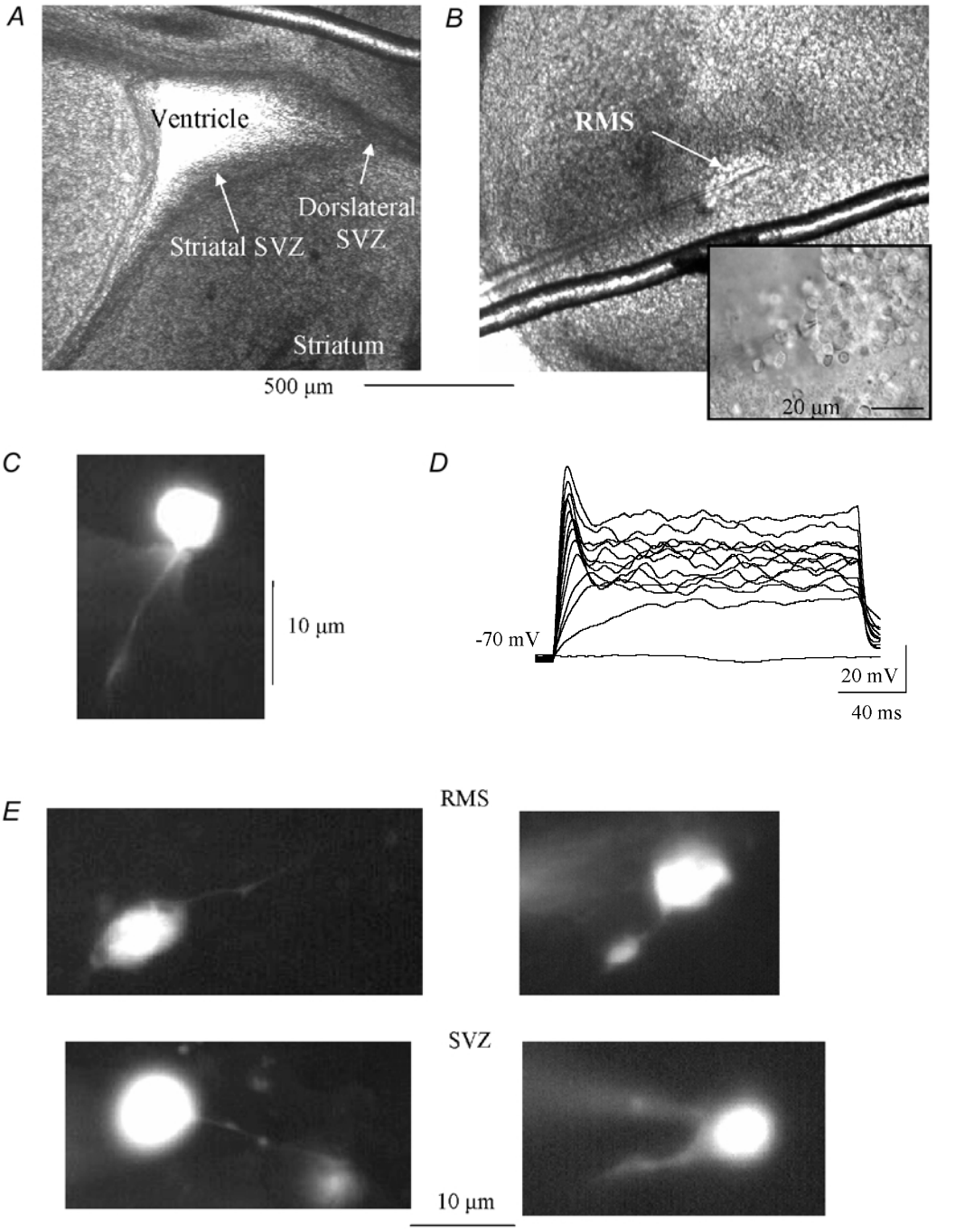

Figure 1. Location of postnatal SVZ cells

A and *B*, low power photographs of corticostriatal slices containing the subventricular zone (SVZ), lining the lateral ventricle (*A*) or the rostral migratory stream (RMS, *B*). The inset in *B* is a high power photograph of progenitors in the RMS. Each picture was taken just before or during recording. *C*, photograph of a LY-filled cell recorded in the SVZ. *D*, voltage traces recorded with the perforated patch-clamp technique in response to 100 pA-increment current injections. *E*, additional photographs of LY-filled cells recorded in the RMS and SVZ that illustrate the diversity in the length and shape of the processes.

mean zero-current V_R (−25.3 ± 8.3 mV, $n = 42$ in the RMS and −23.0 ± 6.2 mV in the SVZ) and R_M (3.5 ± 1.6 MΩ, $n = 44$ in the RMS and 3.5 ± 2.2 MΩ, $n = 46$ in the SVZ). These zero-current resting potential values are close to those published for neuronal progenitors *in vitro* (V_R of −32 mV; Stewart *et al.* 1999). In addition, we found that while the Na^+ conductances of SVZ and RMS progenitors were too low for the generation of current-induced action potentials, the emergence of small spikes in response to current injection may represent an immature action potential (Fig. 1*D*), as previously observed for neuronal progenitors *in vitro* (Stewart *et al.* 1999). These spikes were sensitive to tetrodotoxin, a blocker of voltage-dependent Na^+ channels ($n = 3$, data not shown).

Thus, our morphological and electrophysiological data strongly suggest that recorded cells in the SVZ and RMS belong to the same cell type. In particular, these data suggest that recorded cells are the migrating neuronal progenitors known to proliferate and migrate towards the olfactory bulb in postnatal animals.

Both SVZ and RMS neuronal progenitors contain GABA, the endogenous GABAR ligand, and stain positive for GAD-67

To determine whether progenitors in the studied regions contain GABA and express GAD, immunostainings for GABA and GAD were performed on corticostriatal slices including either the RMS or the SVZ. Progenitors in both the SVZ (Fig. 2*A*, left panel) and RMS (Fig. 2*A*, right panel) stained positive for GABA (green staining). GABA staining

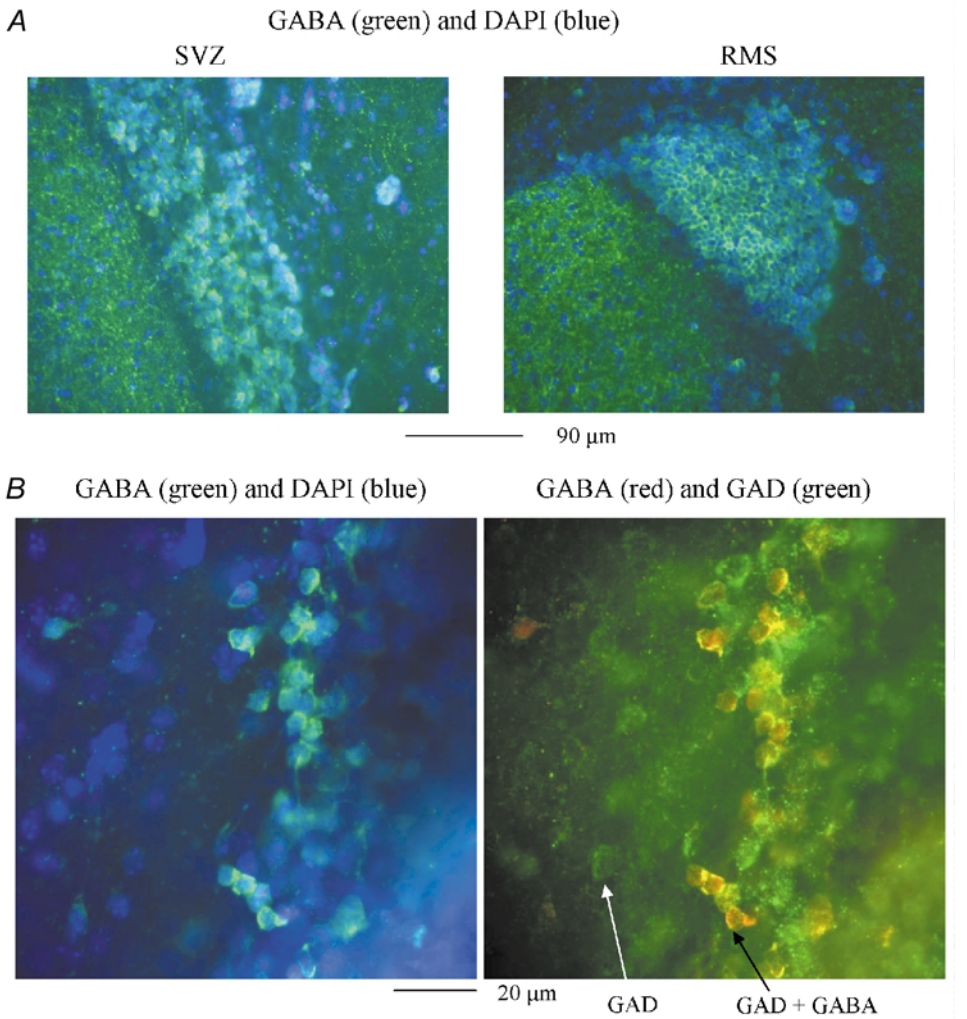

Figure 2. Postnatal neuronal progenitors of the SVZ/RMS contain GABA and GAD

A, low power (× 20 objective) photographs of GABA (green) immunostaining performed in the SVZ (left panel) and in the RMS (right panel). DAPI staining (blue) illustrates that not all the progenitors stain positive for GABA. The staining was performed with 0.1 % Triton X-100 in the blocking solution. In the SVZ slice, the small ventricle collapsed when mounting the slice. *B*, high power (× 100 objective) photographs of GABA (green)/DAPI (blue, left panel) and GABA (red)/GAD (green, right panel) stainings in the same field of view of a rostral SVZ slice. The white arrow points to a cell outside the SVZ that stained positive for GAD but not for GABA. The black arrow points to a SVZ progenitor that stained positive for both GABA and GAD. The staining was performed without any Triton X-100 in the blocking solution.

was found mainly in the cytosol, forming a ring around the dark spherical nucleus. GABA staining outside the SVZ and RMS was essentially punctate as expected for a vesicular staining. Most of the progenitors of the RMS were GABA-positive, indicating that RMS neuronal progenitors contain GABA. In the SVZ, a subpopulation of progenitors was immunopositive for GABA as shown by co-staining for GABA and DAPI (Fig. 2*A* and *B*, left panel). Some of these GABA-positive cells formed clusters or channels, as previously described for neuronal progenitors in the SVZ (Doetsch *et al.* 1997), suggesting that some of the GABA-positive cells were neuronal progenitors. Figure 2*B* (right panel) illustrates co-immunostaining for GABA (red) and GAD-65/67 (green, Stressgene). Every progenitor that contained GABA stained positive for GAD-65/67. We also performed co-staining for GAD-65 and GAD-65/67. Cells in the SVZ/RMS did not stain positive for GAD-65 but stained positive for GAD-65/67 and in the same slice cells in the striatum stained positive for GAD-65, suggesting that neuronal progenitors express GAD-67 (data not shown). Thus, the endogenous ligand of GABARs is present in progenitors of both the RMS and SVZ, suggesting that, if present, GABARs in postnatal neuronal progenitors can be activated by GABA released locally from surrounding cells.

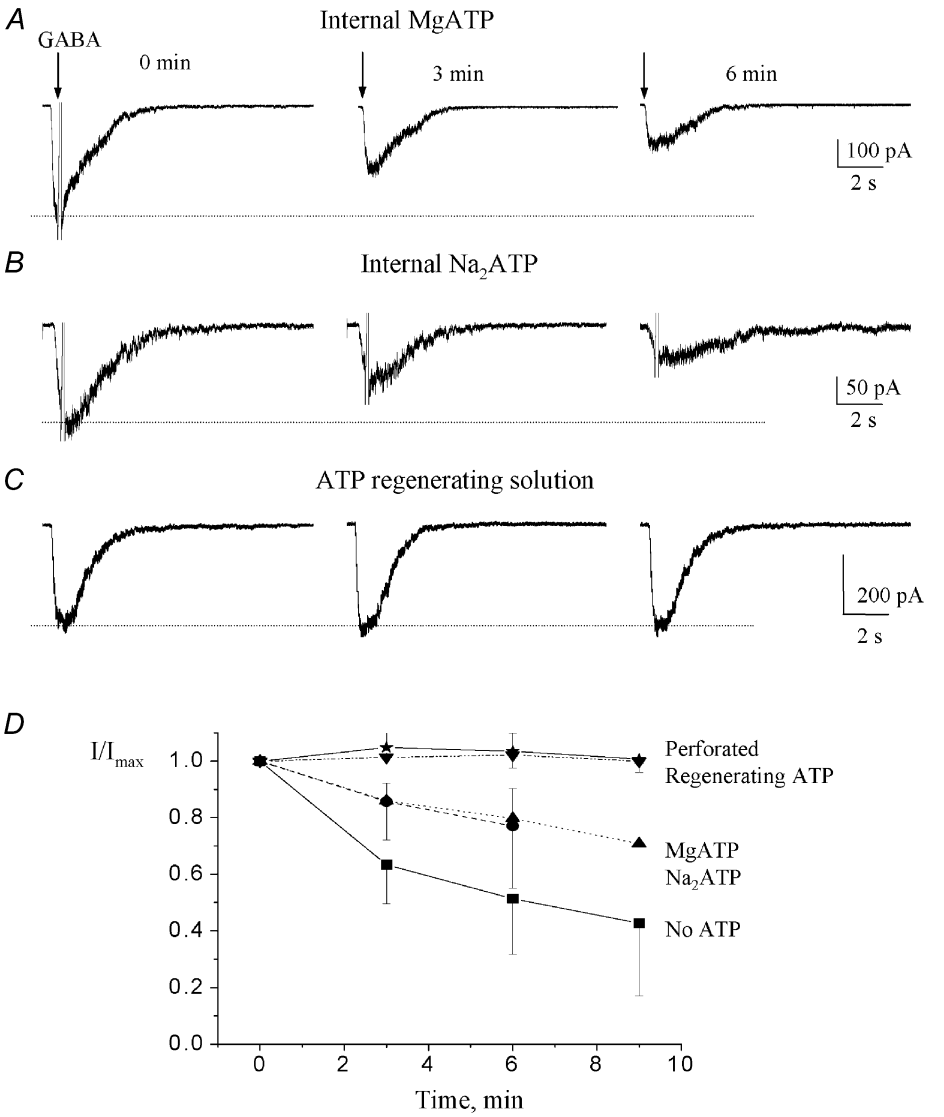

Figure 3. GABA-induced currents display ATP-dependent rundown

A–C, GABA-induced currents recorded at a holding potential of −70 mV. The internal solution contained either MgATP (*A*), Na_2 ATP (*B*) or an ATP-regenerating solution (*C*). GABA was pressure applied at 100 μM every 3 min. *D*, mean (±S.E.M.) normalized GABA-induced current amplitudes plotted against the recording time for each internal solution containing: no ATP, ■; MgATP, ▲; Na_2ATP, ●; a regenerating ATP solution, ▼; gramicidin (perforated), ★. GABA-induced current amplitudes were normalized to the peak current amplitude elicited by the first 100 μM GABA application.

Postnatal neuronal progenitors possess functional $GABA_A$ receptors

Pressure applications of GABA induced transient inward currents in visually and electrophysiologically identified neuronal progenitors recorded at −70 mV. All the progenitors tested responded to GABA. However, the mean peak amplitude of currents induced by 100 μM GABA was variable and ranged in amplitude from −5 to −590 pA (mean of −98.0 ± 116.6 pA, $n = 82$). GABA-induced currents desensitized during GABA application and were accompanied by an increase in noise (Fig. 3), which are two typical characteristics of currents due to ionotropic receptor activation. In addition, GABA-induced currents could be completely and reversibly inhibited by bicuculline (data not shown, Table 1) and picrotoxin (see below, Fig. 6), two $GABA_A$R blockers. This suggests that GABA-induced currents in neuronal progenitors are solely mediated by $GABA_A$R activation.

Rundown. In the absence of internal ATP, the responses evoked by regular (3 min spaced) applications of 100 μM GABA gradually decreased in amplitude (data not shown). The peak current was reduced by 36.6 ± 30.9 % ($n = 6$) between the two first GABA applications. Addition of 4 mM MgATP or Na_2ATP slowed the rundown to a reduction of 14.0 ± 17.3 % ($n = 9$, Fig. 3*A*) and 14.3 ± 27.1 % ($n = 5$, Fig. 3*B* and *C*) between the first and second applications, respectively. The rundown was prevented by inclusion of an ATP-regenerating solution in the pipette solution ($n = 5$, Fig. 3*C*). Similarly, recordings with the perforated patch-clamp technique (see below) abolished the rundown of GABA responses. Figure 3*D* summarizes the effects of the different pipette solutions on the rundown of GABA-induced currents. This graph

Table 1. Mean (± S.D.) effects of various $GABA_A$R modulators on GABA-induced currents in neuronal progenitors

Drugs	$I/I_{control}$	n
Bicuculline (500 μM)*	0.35 ± 0.03	4
Picrotoxin (100 μM)	0.13 ± 0.06	5
Flunitrazepam (1 μM)	1.43 ± 0.07	5
DMCM (1 μM)	0.58 ± 0.09	4
Zolpidem (1 μM)	1.36 ± 0.09	6
Pentobarbital (50 μM)	1.62 ± 0.18	5

*GABA was pressure-applied at 100 μM except for the bicuculline test.

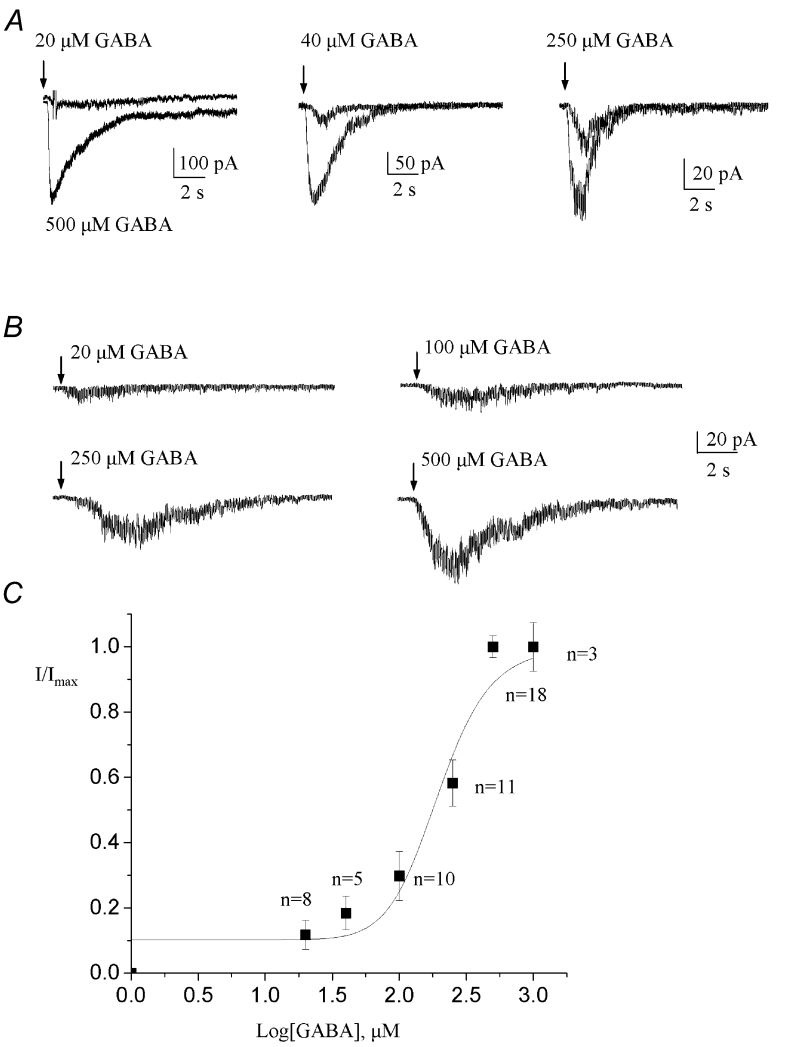

Figure 4. GABA dose–response curve

A, representative examples of currents obtained for a test [GABA] (20, 40 and 250 μM) that was compared to a current induced by 500 μM GABA pressure applied onto the same cell. For each cell, the 500 μM [GABA] was used as a standard. GABA was applied via a θ-glass pipette filled with the test and standard [GABA]. *B*, currents induced by rapid bath applications of GABA at 20, 100, 250 and 500 μM onto the same cell. *C*, GABA-induced current amplitudes normalized to the peak current amplitude elicited by a 500 μM GABA application and plotted as a function of the corresponding [GABA]. A fit to a sigmoidal logistic equation gave an EC_{50} of 196 μM. The cells were recorded at −70 mV with an ATP-containing regenerating internal solution.

illustrates that $GABA_AR$-mediated currents were strongly dependent on the presence of ATP in the pipette solution and that an ATP-regenerating solution is appropriate to study $GABA_ARs$ in neuronal progenitors. Thus, subsequent recordings in the present study were performed with an ATP-regenerating internal solution (except for the perforated patch-clamp experiments).

GABA dose–response curve. Increasing concentrations of GABA (20 μM to 1 mM) were applied on neuronal progenitors via two methods. In the first method, we used θ-glass pipettes to successively pressure apply 500 μM GABA and either 20, 40 or 250 μM GABA from the two respective barrels (Fig. 4*A*). A concentration of 500 μM GABA was found to be saturating and thus used as a standard. The resulting mean dose–response curve was fitted with a logistic equation (see Methods) that gave a mean EC_{50} value of 196.5 μM ($n \geqslant 5$ for each [GABA] tested, data not shown). In each cell tested, the proportion of the test [GABA] response to the saturating [GABA] response was uniform. Because previous studies on $GABA_ARs$ in different cell types have reported EC_{50} values ranging from 0.1 to 200 μM (Ebert *et al.* 1994; Alsbo *et al.* 2001) and because the EC_{50} for GABA was found to be 22 μM for neuronal progenitors *in vitro* (Stewart *et al.* 2002), a second drug application system was employed to confirm our findings. Four different [GABA] were successively and rapidly bath-applied to each cell (Fig. 4*B*, see Methods). The resulting averaged dose–response curve was fitted to a logistic equation (data not shown), which gave a mean EC_{50} of 173.9 μM ($n = 3$, data not shown) similar to that obtained with the previous method of GABA application. Figure 4*C* shows the dose–response curve obtained by pooling data from both methods. A logistic fit of this curve gave a mean EC_{50} value of 196 μM.

Voltage dependence of GABA responses. When the cell membrane was gradually depolarized from −70 to +50 mV, responses to 100 μM GABA decreased progressively in amplitude and reversed close to 0 mV ($n = 3$, Fig. 5*A* and *B*) as expected for a Cl^--carried current in our recording conditions ($E_{Cl} = \sim 2$ mV with internal solution 1 and −4 mV with an ATP-regenerating internal solution). Similar results were obtained when a ramp protocol was applied near the peak of the GABA-induced currents ($n = 16$, Fig. 5*C*).

Picrotoxin sensitivity. The open chloride channel blocker picrotoxin (10–200 μM) was rapidly bath-applied for 10 s before pressure applying GABA. The progressive block of GABA responses by increasing picrotoxin concentrations is shown in Fig. 6*A*. At least four cells were tested for each concentration of picrotoxin. The resulting picrotoxin concentration–inhibition curve was fitted to a sigmoidal logistic function, which gave a mean IC_{50} of 36.0 ± 1.0 μM (Fig. 6*B*). At 100 μM, picrotoxin resulted in a 97 % block of GABA responses (Table 1).

Thus, classical $GABA_ARs$ are present in SVZ and RMS neuronal progenitors recorded in their near-intact environment and account for the GABA responses in these cells.

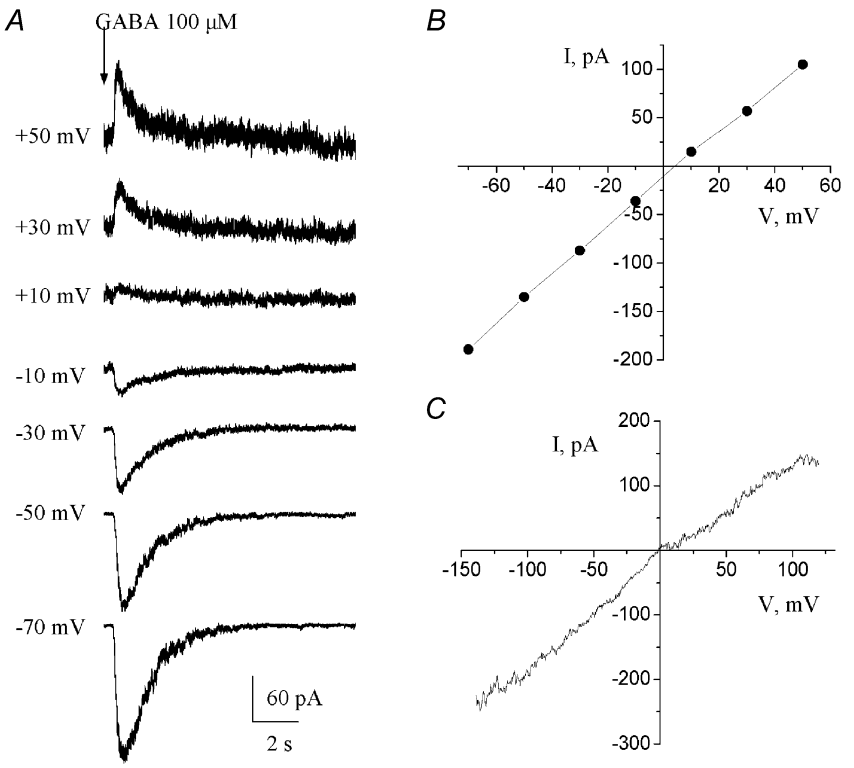

Figure 5. Voltage dependence of GABA-induced currents

A, GABA-induced currents recorded at different holding potentials ranging from −70 to +50 mV. Theses currents reversed at positive membrane potentials. *B*, current–voltage curve of GABA-induced currents for the traces shown in *A*. *C*, current–voltage curve of GABA responses obtained by applying a ramp protocol near the peak of the current (see Fig. 3*A*). These experiments were performed with an ATP-regenerating solution and GABA was pressure applied at 100 μM. In both cases, GABA responses reversed near 0 mV as expected for a Cl^--carried current in our recording conditions.

$GABA_A$Rs in neuronal progenitors are sensitive to Zn^{2+}, benzodiazepines and barbiturates

The divalent metal cation Zn^{2+} has been described as a non-competitive blocker of $GABA_A$Rs (Draguhn *et al.* 1990; McKernan & Whiting, 1996; Horenstein & Akabas, 1998). The inhibitory effects of Zn^{2+} on GABA-induced currents in neuronal progenitor cells were studied by bath applying $ZnCl_2$ (10–400 μM) for at least 30 s prior to a pressure application of 100 μM GABA (Fig. 6*C*). Data from individual cells were normalized, pooled, and fitted to a sigmoidal logistic function (Fig. 6*D*), which gave a mean IC_{50} for Zn^{2+} inhibition of 34.2 ± 1.3 μM (at least three cells tested per dose). A complete block of GABA responses could be obtained with a high concentration of Zn^{2+} (400 μM).

We further tested the effects of benzodiazepines and barbiturates on $GABA_A$Rs in neuronal progenitor cells. The classic benzodiazepine (BZ) agonist flunitrazepam (1 μM) reversibly potentiated responses to 100 μM GABA by 43 % (n = 5/5, Fig. 7*A*). Flunitrazepam was applied ⩾ 15 s before pressure applying GABA. The inverse BZ agonist DMCM (1 μM) uniformly reduced GABA responses by 42 % (n = 4/4, Fig. 7*B*). BZ-sensitive $GABA_A$Rs have been classified into two pharmacological subtypes, BZ_1 (which contains an α1 subunit) and BZ_2 (McKernan & Whiting, 1996). The selective BZ_1 receptor agonist zolpidem (1 μM) reversibly potentiated GABA-induced currents by 36 % (n = 6/6, Fig. 7*C*). This represents a very low sensitivity to zolpidem (EC_{50} of ~100 nM for the BZ_1 receptor, Feigenspan *et al.* 2000), suggesting the absence of the high zolpidem-sensitive α1 subunit. Finally, co-application of the barbiturate pentobarbital (50 μM) also increased GABA responses by 62 %, indicating the presence of a barbiturate-binding site on $GABA_A$Rs in neuronal progenitors (Fig. 7*D*). At this concentration, pentobarbital alone did not induce any inward current. Table 1 summarizes the effects of all these drugs on GABA responses.

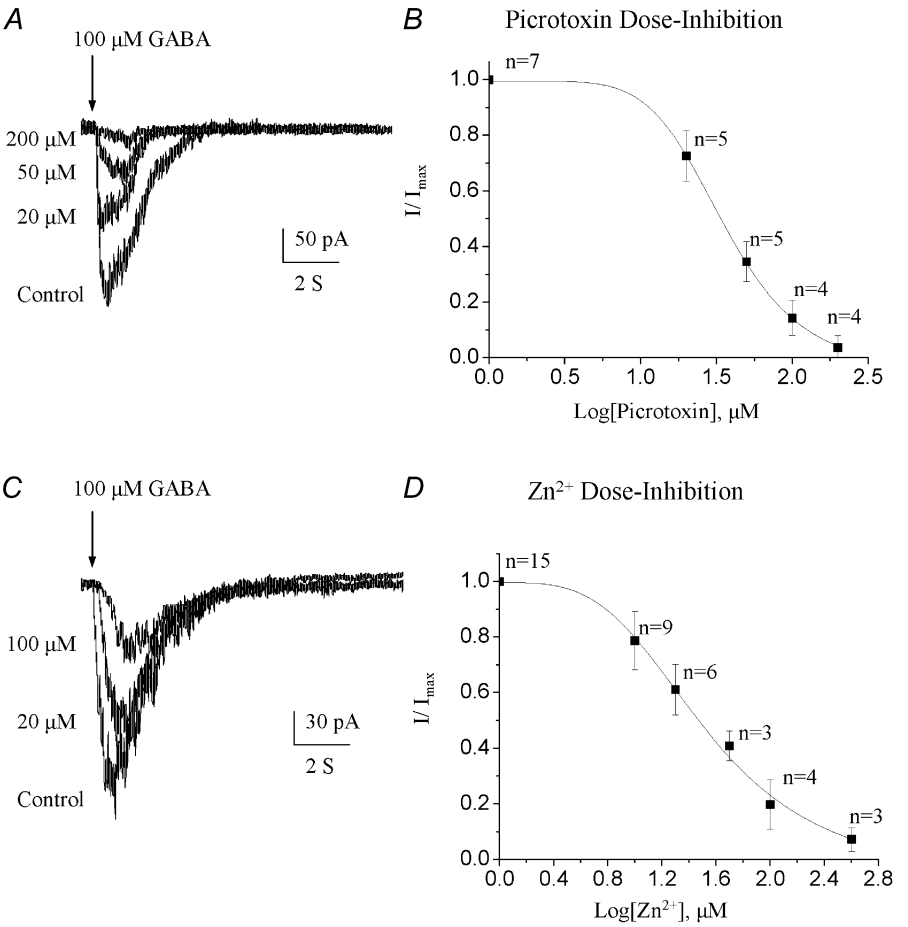

Figure 6. Picrotoxin and Zn^{2+}-sensitivity of GABA-induced currents

A and *C*, superimposed GABA-induced currents under control conditions and in the presence of increasing picrotoxin (*A*) or Zn^{2+} concentrations (*B*). Progenitors were recorded with an ATP-regenerating solution from a holding potential of −70 mV and GABA was pressure applied at 100 μM. *B* and *D*, GABA-induced current amplitudes normalized to the peak amplitude of the control responses and plotted as a function of the corresponding [picrotoxin] (*B*) and [Zn^{2+}] (*D*). A fit to a sigmoidal logistic equation gave an IC_{50} of 346 μM for picrotoxin and 34 μM for Zn^{2+}.

$GABA_A$ receptor activation depolarizes postnatal neuronal progenitor cells

GABA has a well-known inhibitory, hyperpolarizing action on mature neurons. However, GABA has been shown to have an excitatory, depolarizing action on embryonic and immature neurons (Luhmann & Prince, 1991; LoTurco *et al.* 1995; Owens *et al.* 1996; Leinekugel *et al.* 1999). It was also recently shown that GABA depolarizes postnatal neuronal progenitors cultured from the SVZ (Stewart *et al.* 2002). We thus investigated whether GABA would also have an excitatory action on postnatal neuronal progenitors in their near-intact environment (brain slices). Gramicidin perforated patch-clamp recordings were performed to determine the reversal potential (E_{rev}) of GABA responses in a near-physiological $[Cl^-]_i$, which is known to primarily account for the reversal potential of $GABA_A$Rs. Gramicidin is an antibiotic that does not perturb the $[Cl^-]$ gradient across the cell membrane (Myers & Haydon, 1972; Kyrozis & Reichling, 1995). A ramp protocol was applied every 30 s after formation of a gigaseal (Fig. 8*A*). Perforation of the cell membrane started after 15–30 s and stable ramp-induced currents were obtained in 12–15 min (Fig. 8*B*). Postnatal neuronal progenitors had a mean zero-current V_R of -27.7 ± 7.9 mV ($n = 4$) and a mean input resistance of 4.7 ± 2.9 MΩ. Once the ramp-induced currents had reached a steady state, 100 μM GABA was pressure applied and a ramp was applied near the peak of the GABA-induced currents (Fig. 8*C*). A resulting current–voltage relationship is shown in Fig. 8*D*, yielding an E_{rev} close to −40 mV. The mean E_{rev} of GABA responses was -39.3 ± 4.9 mV ($n = 4$, range −33 to −44 mV), which is

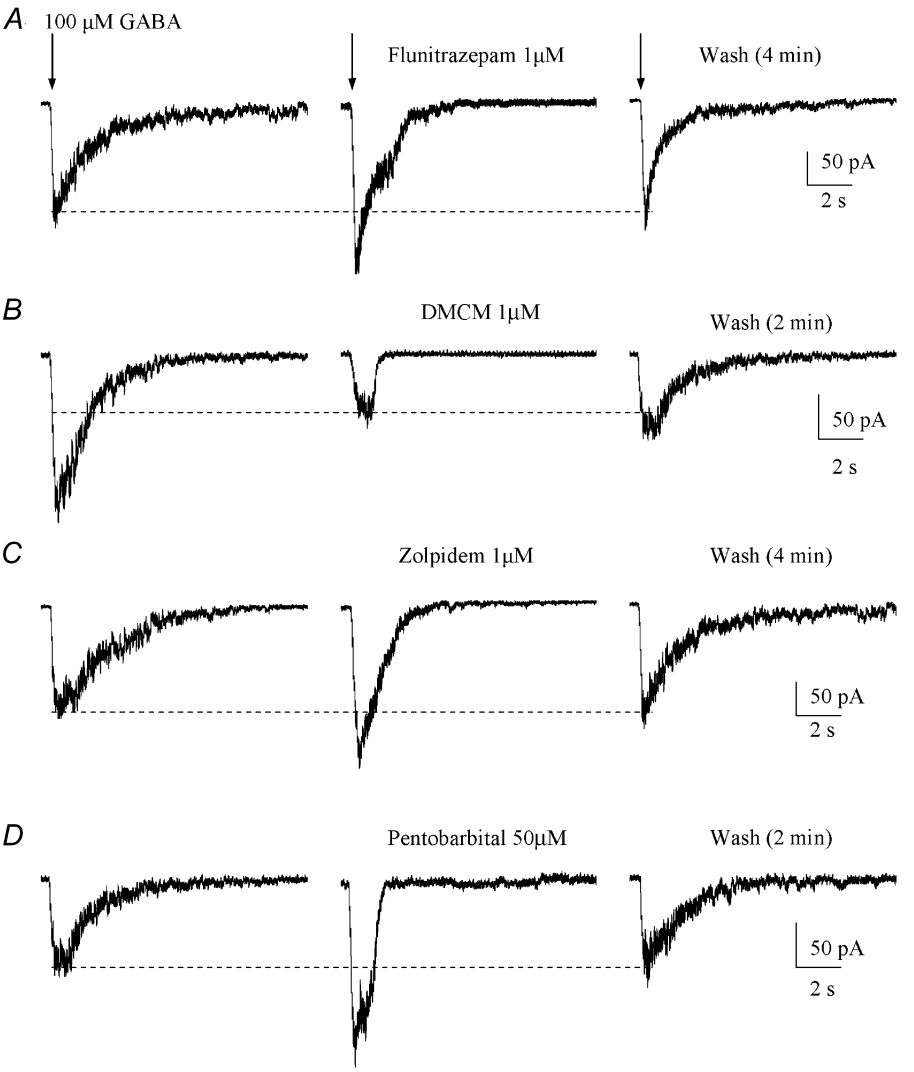

Figure 7. GABA-induced currents are sensitive to benzodiazepines and a barbiturate

A–D, effect of a benzodiazepine agonist (1 μM flunitrazepam), a benzodiazepine inverse agonist (1 μM DMCM) , a BZ1-selective agonist (1 μM zolpidem) and a barbiturate (50 μM pentobarbital) on GABA-induced currents. Each GABA receptor modulator was applied by a rapid bath application system and GABA was pressure applied at 100 μM. Neuronal progenitors were recorded with an ATP-regenerating internal solution and held at −70 mV.

more hyperpolarized than the cell zero-current resting potential (range −20 to −36 mV, $n = 4$). Based on the Nernst equation, the calculated $[Cl^-]_i$ in neuronal progenitors would be 29.4 ± 5.2 mM. Considering that $GABA_A$Rs are also permeable to HCO_3^-, this would give a mean $[Cl^-]_i$ of 26.7 ± 6.0 mM, using the equation:

$$E_{rev} = (RT/F)\ln[([Cl^-]_e + 0.2[HCO_3^-]_e)/([Cl^-]_i + 0.2[HO_3^-]_i)]$$

with a HCO_3^--to-Cl^- permeability ratio of 0.2 (Bormann *et al.* 1987) and a $[HCO3^-]_i$ of 16 mM (Staley *et al.* 1995). Under current clamp, GABA depolarized neuronal progenitors recorded at −70 mV and around −50 mV (Fig. 8*E*), and hyperpolarized neuronal progenitors recorded at their zero-current resting potentials (−25 mV in Fig. 8*E*, E_{rev} of GABA-induced currents was −33 mV in this cell). However, the zero-current resting potential of

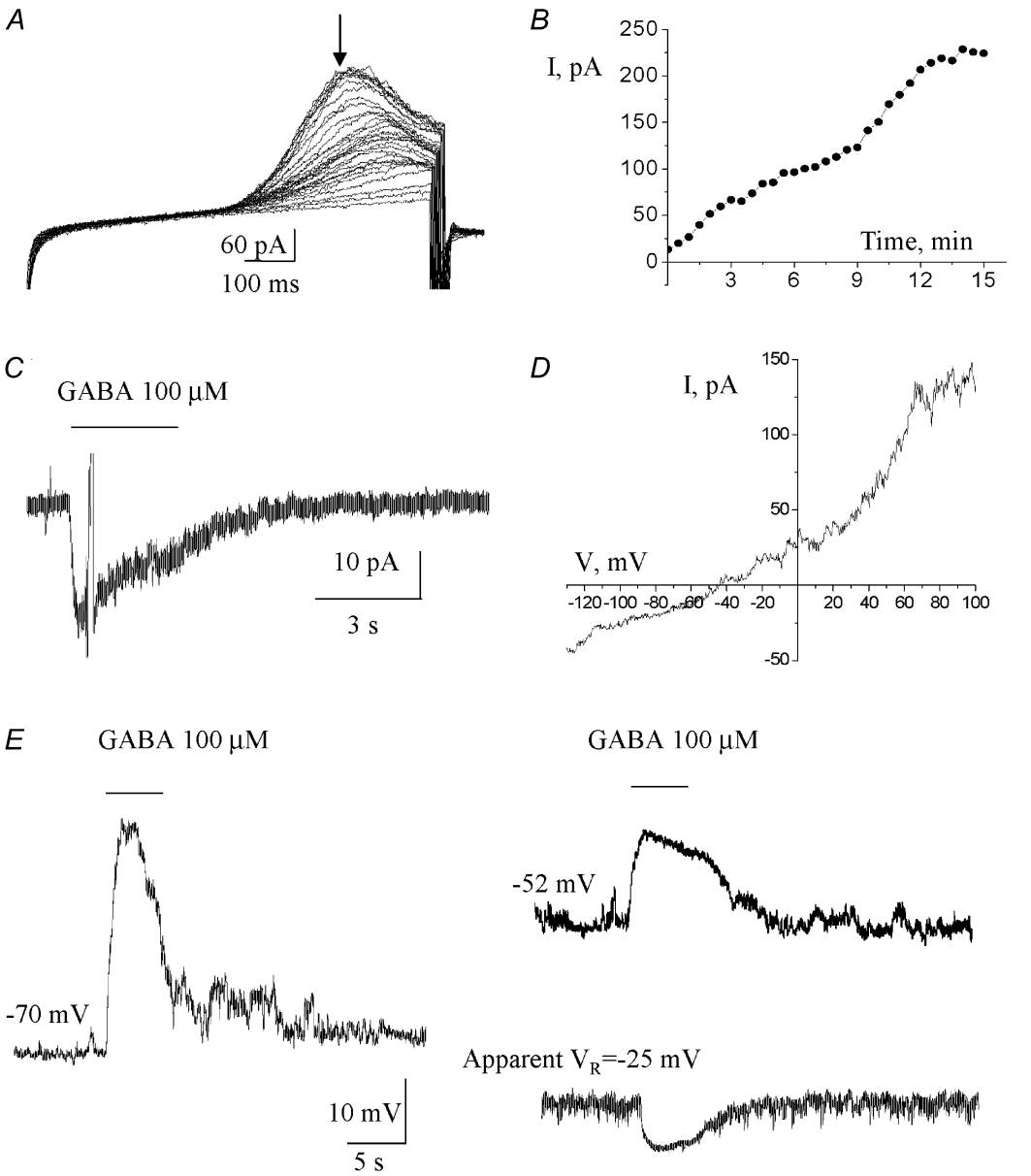

Figure 8. GABA hyperpolarizes postnatal neuronal progenitors as shown by gramicidin perforated patch-clamp recordings

A, currents induced by a ramp protocol applied every 30 s immediately after formation of a gigaseal. *B*, current amplitudes measured at the time point indicated by the arrow in *A* and plotted as a function of the recording time. The currents reached a steady state in about 12–15 min following the gigaseal formation. *C*, 100 μM GABA-induced current obtained in a progenitor recorded with the gramicidin perforated patch-clamp technique. A ramp protocol was applied near the peak of the current. *D*, current–voltage curve of the GABA response shown in *C*. *E*, membrane depolarization and hyperpolarization induced by GABA in a postnatal progenitor recorded at −70 and −52 mV, and at its zero-current resting membrane potential of −25 mV, respectively. Recordings were obtained with the perforated patch-clamp technique.

neuronal progenitors probably does not represent the true resting potential of these cells because neuronal progenitors have a very high input resistance (close to 4 GΩ) and seal resistances were usually less than 10 GΩ. Thus, it is likely that the seal introduces a significant conductance that probably depolarizes recorded cells (Pongracz *et al.* 1991). We thus estimated the resting potential of neuronal progenitors with an alternative method that is more appropriate for these cells. We performed cell-attached recordings and used the reversal potential of K^+ channels as a monitor of the cell membrane potential, as previously described for hippocampal interneurons (Verheugen *et al.* 1999; Fricker *et al.* 1999). To activate K^+ channels, voltage ramps from −140 to +200 mV ($-V_{pip}$, Fig. 9*A*) were repeated at 0.5 Hz without any significant inactivation of K^+ channels. At the K^+ channel reversal, the cell membrane potential, which at rest gives an estimate of the cell resting potential, was −61.3 ± 2.9 mV ($n = 3$, Fig. 9*A*). This finding indicates that GABA should depolarize neuronal progenitors at rest. To confirm our findings, we estimated the resting potential of hippocampal pyramidal cells as reported by Fricker *et al.* (1999). The estimated resting potentials were between −82 and −88 mV ($n = 4$) similar to previously reported values (Fricker *et al.* 1999). After obtaining data in the cell-attached mode we recorded these neurons in the whole-cell configuration that gave resting membrane potentials (zero current level) between −76 and −79 mV. This difference in resting potentials between the two

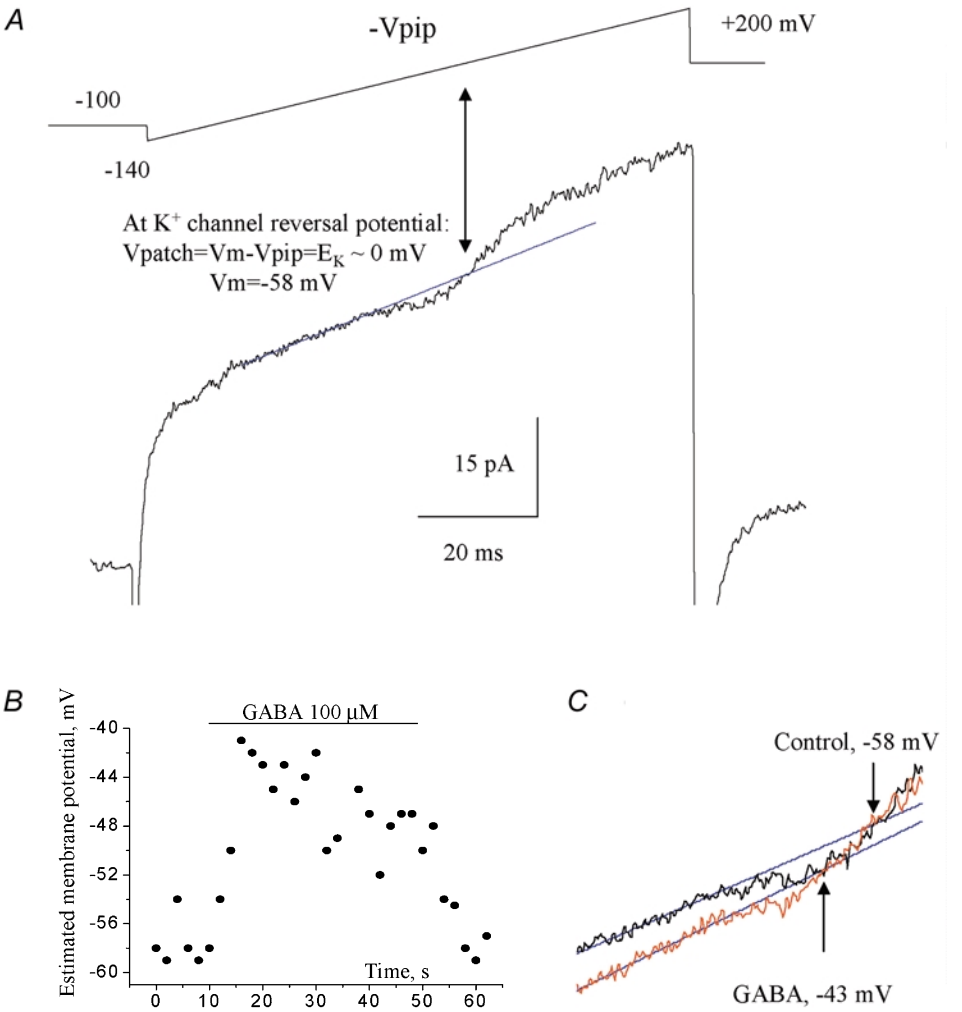

Figure 9. Measurements of GABA action on the cell membrane potential using cell-attached recordings

A, a cell-attached record in response to a depolarizing ramp command (shown above the trace) from −140 to +200 mV ($-V_{pip}$). The holding potential ($-V_{pip}$) was −100 mV with respect to the cell membrane potential. Voltage-gated K^+ currents activated by the depolarizing voltage ramp were initially inward, and then reversed to become outward. E_K was determined from the intersection of the fit (straight line) to the linear leak and the K^+ current. The cell resting membrane potential was measured from the reversal of cell-attached K^+ currents. *B*, plot of the cell membrane potential measured as shown in *A* against the recording time. GABA was pressure applied for 40 s as indicated by the bar. *C*, determination of K^+ current reversal before and during GABA application (6 s after the start of the application).

modes is also consistent with previous studies (Verheugen *et al.* 1999; Fricker *et al.* 1999). We then tested the action of GABA on the cell membrane potential using cell-attached recordings of neuronal progenitors. During pressure application of 100 μM GABA for 40 s, the cell membrane potential was depolarized to -41.7 ± 2.3 mV ($n = 3$, Fig. 9*B* and *C*), confirming that GABA depolarizes postnatal neuronal progenitors in their near-intact environment.

DISCUSSION

For the first time, this study reports the presence and properties of functional $GABA_A$ receptors in postnatal SVZ and RMS neuronal progenitors recorded in their near intact environment (brain slices). More specifically, our data show that: (1) neuronal progenitors possess functional benzodiazepine and zinc-sensitive $GABA_A$Rs that display an ATP-dependent rundown and a low sensitivity to GABA, and (2) GABA has a depolarizing action on postnatal neuronal progenitors similar to that previously reported in embryonic and neonatal immature neurons.

Recorded cells in the SVZ/RMS are neuronal progenitors that contain GABA

Recorded cells in the RMS and anterior SVZ were identified as neuronal progenitors based on their location, morphology and immature electrophysiological characteristics. First, 60–80 % of the anterior SVZ and the RMS consists of neuronal progenitors (Luskin, 1993; McKernan & Whiting, 1996; Doetsch *et al.* 1997), resulting in a high probability of recording from neuronal progenitors. Second, Lucifer Yellow-filled cells resembled migrating progenitors committed to either a neuronal or glial lineage (Levison *et al.* 1993; Doetsch *et al.* 1997; Kakita & Goldman, 1999). More specifically, cells recorded in this study in either the RMS or the SVZ displayed a morphology similar to that of neuronal progenitors that migrate to the olfactory bulb via the RMS (Doetsch *et al.* 1997; Stewart *et al.* 1999). In addition, the remaining 20–30 % of the cells described in the RMS have a morphology characterized by more developed processes, which is different from that reported in the cells recorded in this study (Doetsch *et al.* 1997; Gritti *et al.* 2002). Third, RMS and SVZ cells displayed identical electrophysiological properties, characterized in particular by a depolarized zero-current resting membrane potential and the lack of fast action potentials as previously reported for postnatal neuronal progenitors cultured from the anterior SVZ (Stewart *et al.* 1999). Together, these data strongly suggest that cells recorded in the SVZ and RMS were neuronal progenitors.

Most of the postnatal progenitors of the RMS were GABA-positive, indicating that RMS neuronal progenitors contain GABA. A subpopulation of SVZ progenitors was immunopositive for GABA. Some of these GABA-positive cells formed clusters, as previously described for neuronal progenitors in the SVZ (Doetsch *et al.* 1997), suggesting that some of the SVZ neuronal progenitors contain GABA. In addition, every progenitor that contained GABA stained positive for its synthesizing enzyme, GAD. This is consistent with the study by Stewart *et al.* (2002), which showed that postnatal neuronal progenitors cultured from the anterior SVZ contain GABA and GAD. Thus, the presence of GABA in postnatal SVZ and RMS progenitors supports the concept that GABA released by neuronal progenitors and eventually by other surrounding cells is a local factor that can signal to neuronal progenitors by activating $GABA_A$Rs.

Postnatal neuronal progenitors express functional $GABA_A$ receptors that display a strong rundown and low sensitivity to GABA

GABA induced inward currents that were voltage dependent and fully blocked by picrotoxin, a $GABA_A$R blockers, identifying these currents as $GABA_A$R-mediated responses in postnatal neuronal progenitors. No apparent $GABA_B$R-mediated currents were detected.

ATP-dependent rundown. In our recordings, GABA responses displayed a strong rundown that was not fully prevented by inclusion of ATP in the patch pipette but required an ATP-regenerating solution. Such a rundown was apparently not present in neuronal progenitors cultured from the anterior SVZ (Stewart *et al.* 2002), suggesting either a different subunit composition of the $GABA_A$Rs or a different intracellular machinery to maintain cell surface expression of these receptors (Huang & Dillon, 1998; Connolly *et al.* 1999). For example, phosphorylation by PKC and protein tyrosine kinase can regulate the cell surface levels of $GABA_A$Rs.

GABA sensitivity. In our study, the EC_{50} of $GABA_A$Rs in mouse neuronal progenitors (196 μM) is much higher than that found in neuronal progenitors cultured from the rat anterior SVZ (22 μM; Stewart *et al.* 2002). Although recorded cells were located at the slice surface or one cell layer inside the slice ($\leqslant 20$ μM deep) and we used two application systems to ascertain our findings, it is possible that a slower exchange rate in slices than in culture accounts for the higher EC_{50} obtained in our study. It is also possible that our recording conditions, in particular the presence of an ATP-regenerating system, lower the receptor sensitivity to GABA, probably via phosphorylation as was previously shown with the inclusion of MgATP in the pipette solution (Gyenes *et al.* 1994). Alternatively, different $GABA_A$R subunit combinations are known to have different sensitivities to GABA (EC_{50} values ranging from 0.1 to 200 μM; Ebert *et al.* 1994; Alsbo *et al.* 2001). It is thus possible that neuronal progenitors in their near-intact environment express $GABA_A$Rs with a different subunit combination than that of $GABA_A$Rs expressed in cultured neuronal progenitors.

In fact, this is in agreement with the difference in rundown observed in cultured and *in situ* recordings.

Zn^{2+} and benzodiazepine sensitivities of $GABA_A$ receptors in neuronal progenitors

$GABA_AR$-mediated currents display a low sensitivity to Zn^{2+} (IC_{50} of 34 μM) in all neuronal progenitors tested. Zn^{2+} sensitivity is known to depend on the $GABA_AR$ subunit composition. Previous studies have reported that $GABA_ARs$ consisting of only α and β subunits are highly sensitive to Zn^{2+} ($IC_{50} < 2$ μM; Draguhn *et al.* 1990; Horenstein & Akabas, 1998) while the presence of a γ subunit greatly lowered the Zn^{2+} sensitivity of $GABA_ARs$ (IC_{50} ~1 mM, Draguhn *et al.* 1990; Horenstein & Akabas, 1998; Feigenspan *et al.* 2000; Stewart *et al.* 2002). Thus, in neuronal progenitors the low sensitivity to Zn^{2+} suggests the presence of a γ subunit in their $GABA_ARs$. This is in agreement with the reported presence of a γ2S subunit in cultured SVZ neuronal progenitors (Stewart *et al.* 2002). Nevertheless, to clearly demonstrate the presence of a γ2 subunit in neuronal progenitors, it would be necessary to perform immunostaining or RT-PCR for the γ2 subunit in both the SVZ and the RMS of the olfactory bulb, which is beyond the scope of this study.

In order to further characterize $GABA_ARs$ in neuronal progenitors, we tested the effects of BZ agonists (flunitrazepam and zolpidem) and an inverse BZ agonist (DMCM). These allosteric regulators modulated GABA responses in all neuronal progenitors tested. However, the efficacy of receptor modulation, which is known to depend primarily on the subunit combination of the $GABA_AR$ (McKernan & Whiting, 1996; Hevers & Luddens, 1998; Whiting *et al.* 1999), varied greatly between drugs, making it possible to speculate on the types of subunits present in these neuronal progenitors. These changes in GABA responses observed in the presence of flunitrazepam and DMCM (−43 % and +58 %, respectively) lie within the expected ranges for a BZ-sensitive receptor, confirming the presence of a γ2 subunit in $GABA_ARs$ in neuronal progenitors (Pritchett *et al.* 1989). In contrast, zolpidem in our study, although uniformly potentiating GABA responses, had a very low efficacy (36 % increase at 1 μM). Zolpidem is a BZ_1-selective agonist with high affinity for the α1 subunit (EC_{50}: 20–100 nM, McKernan & Whiting, 1996; Feigenspan *et al.* 2000) and low affinities for the α2 and α3 subunits (EC_{50}: 300–400 nM). Thus our results suggest that $GABA_ARs$ in neuronal progenitors do not possess an α1 subunit, which is in agreement with the absence of an α1 subunit in cultured neuronal progenitors (Stewart *et al.* 2002).

GABA depolarizes postnatal neuronal progenitors

In our study we found that GABA depolarized postnatal neuronal progenitors in the SVZ/RMS recorded with the cell-attached and the gramicidin perforated patch-clamp technique. This effect of GABA on postnatal progenitors is similar to that previously reported in embryonic and neonatal immature neurons (Mueller *et al.* 1983; LoTurco *et al.* 1995; Owens *et al.* 1996; Leinekugel *et al.* 1999; Stewart *et al.* 2002). In immature neurons, including neonatal neurons (Mueller *et al.* 1983; Leinekugel *et al.* 1999) and embryonic neurons (LoTurco *et al.* 1995; Owens *et al.* 1996), GABA responses have been shown to reverse between −30 and −40 mV, close to the values (−39 mV) obtained in our studies. However, GABA responses were found to reverse at a more hyperpolarized membrane potential in our study than that (−17 mV) reported in cultured SVZ cells (Stewart *et al.* 2002). The discrepancy in the reversal potential of GABA responses on postnatal SVZ neuronal progenitors could be due to a difference in $[Cl^-]_i$ in neuronal progenitors studied in slices or in cultures. Alternatively, it seems quite possible that methodological differences such as the use of a bicarbonate-buffered solution in our study rather than a Hepes-buffered external solution may explain the difference in E_{rev}. If Cl^--bicarbonate exchange were involved in regulating the $[Cl^-]_i$ in SVZ progenitors, then exposure to 25 mM bicarbonate would indeed lower internal $[Cl^-]$ producing a more negative E_{rev}. Regarding GABA action, we used an alternative method that allowed us to obtain a better estimate of the cell resting potential and to determine the action of GABA on the membrane potential. This method consisted of using the reversal potential of K^+ channels in cell-attached records as a monitor of the cell membrane potential (Verheugen *et al.* 1995, 1999; Fricker *et al.* 1999). It was possible to use this method because neuronal progenitors express delayed rectifying K^+ channels (D. D. Wang and A. Bordey, unpublished observation). This method allowed precise measurements of the cell membrane potential without disturbing the intracellular milieu. While we obtained a mean resting potential of −27 mV with perforated patch-clamp recordings, the cell-attached method gave a significantly more hyperpolarized resting potential of −60 mV. Because we assumed that the intracellular $[K^+]$ is close to 155 mV, based on the value reported for other cell types, we might introduce a small error in the measurement of the resting potential. However, as mentioned by Verheugen *et al.* (1999), an error of 15 mM in the intracellular $[K^+]$ would result in an error < 3 mV in the membrane potential measurement. The discrepancy between V_R measured with cell-attached and whole-cell recordings can be easily explained by the contribution of a relatively large seal conductance (between 0.1 and 0.2 pS) by comparison with the seal input conductance (about 0.25 pS). Such a seal conductance would significantly depolarize these cells (Pongracz *et al.* 1991). Thus, while GABA appears to be hyperpolarizing at the zero-current resting potential, it is depolarizing at the resting potential estimated with cell-attached measurements. This finding was confirmed by studying the action of GABA on the

membrane potential monitored with cell-attached recordings.

The depolarizing action of GABA on the resting potential may have important implications for the role of GABA on postnatal neuronal progenitor behaviour during their tangential migration toward the olfactory bulb. Previous studies have shown that GABA decreases the proliferation and promotes the migration of embryonic neurons, probably via a depolarization-based mechanism (LoTurco *et al.* 1995; Behar *et al.* 1996; Antonopoulos *et al.* 1997; Behar *et al.* 1998; Haydar *et al.* 2000; Behar *et al.* 2000). In addition, GABA-mediated hyperpolarization may prevent cell migration by decreasing the driving force for Ca^{2+} influx or promote migration by opening potential voltage-dependent Ca^{2+} channels. Although it is difficult to anticipate the consequences of GABA action on the proliferation/migration of neuronal progenitors, GABA might have important functions on the behaviour of postnatal neuronal progenitors during their tangential migration toward the olfactory bulb.

Overall, our study demonstrates that postnatal neuronal progenitors of the SVZ/RMS contain GABA and are depolarized by GABA, which may constitute the basis for an autocrine/paracrine signal among neuronal progenitors to regulate the dynamics of neuronal progenitor proliferation/migration.

REFERENCES

Alsbo CW, Kristiansen U, Moller F, Hansen SL & Johansen FF (2001). $GABA_A$ receptor subunit interactions important for benzodiazepine and zinc modulation: a patch-clamp and single cell RT-PCR study. *Eur J Neurosci* **13**, 1673–1682.

Alvarez-Buylla A & Temple S (1998). Stem cells in the developing and adult nervous system. *J Neurobiol* **36**, 105–110.

Antonopoulos J, Pappas IS & Parnavelas JG (1997). Activation of the $GABA_A$ receptor inhibits the proliferative effects of bFGF in cortical progenitor cells. *Eur J Neurosci* **9**, 291–298.

Baker H, Liu N, Chun HS, Saino S, Berlin R, Volpe B & Son JH (2001). Phenotypic differentiation during migration of dopaminergic progenitor cells to the olfactory bulb. *J Neurosci* **21**, 8505–8513.

Barker JL, Behar T, Li YX, Liu QY, Ma W, Maric D, Maric I, Schaffner AE, Serafini R, Smith SV, Somogyi R, Vautrin JY, Wen XL & Xian H (1998). GABAergic cells and signals in CNS development. *Perspect Dev Neurobiol* **5**, 305–322.

Behar TN, Li YX, Tran HT, Ma W, Dunlap V, Scott C & Barker JL (1996). GABA stimulates chemotaxis and chemokinesis of embryonic cortical neurons via calcium-dependent mechanisms. *J Neurosci* **16**, 1808–1818.

Behar TN, Schaffner AE, Scott CA, Greene CL & Barker JL (2000). GABA receptor antagonists modulate postmitotic cell migration in slice cultures of embryonic rat cortex. *Cereb Cortex* **10**, 899–909.

Behar TN, Schaffner AE, Scott CA, O'Connell C & Barker JL (1998). Differential response of cortical plate and ventricular zone cells to GABA as a migration stimulus. *J Neurosci* **18**, 6378–6387.

Bordey A, Lyons SA, Hablitz JJ & Sontheimer H (2001). Electrophysiological characteristics of reactive astrocytes in experimental cortical dysplasia. *J Neurophysiol* **85**, 1719–1731.

Bordey A & Sontheimer H (1997). Postnatal development of ionic currents in rat hippocampal astrocytes in situ. *J Neurophysiol* **78**, 461–477.

Bordey A & Sontheimer H (2000). Ion channel expression by astrocytes in situ: comparison of different CNS regions. *Glia* **30**, 27–38.

Bormann J, Hamill OP & Sakmann B (1987). Mechanism of anion permeation through channels gated by glycine and gamma-aminobutyric acid in mouse cultured spinal neurones. *J Physiol* **385**, 243–286.

Connolly CN, Kittler JT, Thomas P, Uren JM, Brandon NJ, Smart TG & Moss SJ (1999). Cell surface stability of gamma-aminobutyric acid type A receptors. Dependence on protein kinase C activity and subunit composition. *J Biol Chem* **274**, 36565–36572.

Coskun V & Luskin MB (2002). Intrinsic and extrinsic regulation of the proliferation and differentiation of cells in the rodent rostral migratory stream. *J Neurosci Res* **69**, 795–802.

Doetsch F, Caille I, Lim DA, Garcia-verdugo JM & Alvarez-Buylla A (1999). Subventricular zone astrocytes are neural stem cells in the adult mammalian brain. *Cell* **97**, 703–716.

Doetsch F, Garcia-Verdugo JM & Alvarez-Buylla A (1997). Cellular composition and three-dimensional organization of the subventricular germinal zone in the adult mammalian brain. *J Neurosci* **17**, 5046–5061.

Draguhn A, Verdorn TA, Ewert M, Seeburg PH & Sakmann B (1990). Functional and molecular distinction between recombinant rat $GABA_A$ receptor subtypes by Zn^{2+}. *Neuron* **5**, 781–788.

Ebert B, Wafford KA, Whiting PJ, Krogsgaard-Larsen P & Kemp JA (1994). Molecular pharmacology of gamma-aminobutyric acid type A receptor agonists and partial agonists in oocytes injected with different alpha, beta, and gamma receptor subunit combinations. *Mol Pharmacol* **46**, 957–963.

Edwards FA & Konnerth A (1992). Patch-clamping cells in sliced tissue preparations. *Methods Enzymol* **207**, 208–222.

Feigenspan A, Gustincich S & Raviola E (2000). Pharmacology of GABA(A) receptors of retinal dopaminergic neurons. *J Neurophysiol* **84**, 1697–1707.

Forscher P & Oxford GS (1985). Modulation of calcium channels by norepinephrine in internally dialyzed avian sensory neurons. *J Gen Physiol* **85**, 743–763.

Fricker D, Verheugen JA & Miles R (1999). Cell-attached measurements of the firing threshold of rat hippocampal neurones. *J Physiol* **517**, 791.

Fueshko SM, Key S & Wray S (1998). GABA inhibits migration of luteinizing hormone-releasing hormone neurons in embryonic olfactory explants. *J Neurosci* **18**, 2560–2569.

Garcia-Verdugo JM, Doetsch F, Wichterle H, Lim DA & Alvarez-Buylla A (1998). Architecture and cell types of the adult subventricular zone: in search of the stem cells. *J Neurobiol* **36**, 234–248.

Gritti A, Bonfanti L, Doetsch F, Caille I, Alvarez-Buylla A, Lim DA, Galli R, Verdugo JM, Herrera DG & Vescovi AL (2002). Multipotent neural stem cells reside into the rostral extension and olfactory bulb of adult rodents. *J Neurosci* **22**, 437–445.

Gyenes M, Wang Q, Gibbs TT & Farb DH (1994). Phosphorylation factors control neurotransmitter and neuromodulator actions at the gamma-aminobutyric acid type A receptor. *Mol Pharmacol* **46**, 542–549.

Haydar TF, Wang F, Schwartz ML & Rakic P (2000). Differential modulation of proliferation in the neocortical ventricular and subventricular zones. *J Neurosci* **20**, 5764–5774.

Hevers W & Luddens H (1998). The diversity of $GABA_A$ receptors. Pharmacological and electrophysiological properties of $GABA_A$ channel subtypes. *Mol Neurobiol* **18**, 35–86.

Hille, B. (1992). *Ionic Channels of Excitable Membranes*, Introduction, pp. 1–20. Sinauer Associates Inc., Sunderland, MA, USA.

Horenstein J & Akabas MH (1998). Location of a high affinity Zn^{2+} binding site in the channel of alpha1beta1 gamma-aminobutyric acidA receptors. *Mol Pharmacol* **53**, 870–877.

Huang RQ & Dillon GH (1998). Maintenance of recombinant type A gamma-aminobutyric acid receptor function: role of protein tyrosine phosphorylation and calcineurin. *J Pharmacol Exp Ther* **286**, 243–255.

Kakita A & Goldman JE (1999). Patterns and dynamics of SVZ cell migration in the postnatal forebrain: monitoring living progenitors in slice preparations. *Neuron* **23**, 461–472.

Kyrozis A & Reichling DB (1995). Perforated-patch recording with gramicidin avoids artifactual changes in intracellular chloride concentration. *J Neurosci Methods* **57**, 27–35.

Leinekugel X, Khalilov I, McLean H, Caillard O, Gaiarsa JL, Ben Ari Y & Khazipov R (1999). GABA is the principal fast-acting excitatory transmitter in the neonatal brain. *Adv Neurol* **79**, 189–201.

Levison SW, Chuang C, Abramson BJ & Goldman JE (1993). The migrational patterns and developmental fates of glial precursors in the rat subventricular zone are temporally regulated. *Development* **119**, 611–622.

Levison SW & Goldman JE (1997). Multipotential and lineage restricted precursors coexist in the mammalian perinatal subventricular zone. *J Neurosci Res* **48**, 83–94.

Lois C, Garcia-Verdugo JM & Alvarez-Buylla A (1996). Chain migration of neuronal precursors. *Science* **271**, 978–981.

Loturco JJ, Owens DF, Heath MJ, Davis MB & Kriegstein AR (1995). GABA and glutamate depolarize cortical progenitor cells and inhibit DNA synthesis. *Neuron* **15**, 1287–1298.

Luhmann HJ & Prince DA (1991). Postnatal maturation of the GABAergic system in rat neocortex. *J Neurophysiol* **65**, 247–263.

Luskin MB (1993). Restricted proliferation and migration of postnatally generated neurons derived from the forebrain subventricular zone. *Neuron* **11**, 173–189.

Luskin MB (1998). Neuroblasts of the postnatal mammalian forebrain: their phenotype and fate. *J Neurobiol* **36**, 221–233.

MacDonald JF, Mody I & Salter MW (1989). Regulation of *N*-methyl-D-aspartate receptors revealed by intracellular dialysis of murine neurones in culture. *J Physiol* **414**, 17–34.

McKernan RM & Whiting PJ (1996). Which $GABA_A$-receptor subtypes really occur in the brain? *Trends Neurosci* **19**, 139–143.

Momma S, Johansson CB & Frisen J (2000). Get to know your stem cells. *Curr Opin Neurobiol* **10**, 45–49.

Mueller AL, Chesnut RM & Schwartzkroin PA (1983). Actions of GABA in developing rabbit hippocampus: an *in vitro* study. *Neurosci Lett* **39**, 193–198.

Murase S & Horwitz AF (2002). Deleted in colorectal carcinoma and differentially expressed integrins mediate the directional migration of neural precursors in the rostral migratory stream. *J Neurosci* **22** , 3568–3579.

Myers VB & Haydon DA (1972). Ion transfer across lipid membranes in the presence of gramicidin A. II. The ion selectivity. *Biochim Biophys Acta* **274**, 313–322.

Owens DF, Boyce LH, Davis MB & Kriegstein AR (1996). Excitatory GABA responses in embryonic and neonatal cortical slices demonstrated by gramicidin perforated-patch recordings and calcium imaging. *J Neurosci* **16** , 6414–6423.

Pongracz F, Firestein S & Shepherd GM (1991). Electrotonic structure of olfactory sensory neurons analyzed by intracellular and whole cell patch techniques. *J Neurophysiol* **65**, 747–758.

Pritchett DB, Luddens H & Seeburg PH (1989). Type I and type II $GABA_A$-benzodiazepine receptors produced in transfected cells. *Science* **245**, 1389–1392.

Shihabuddin LS, Palmer TD & Gage FH (1999). The search for neural progenitor cells: prospects for the therapy of neurodegenerative disease. *Mol Med Today* **5**, 474–480.

Staley KJ, Soldo BL & Proctor WR (1995). Ionic mechanisms of neuronal excitation by inhibitory $GABA_A$ receptors. *Science* **269**, 977–981.

Stewart RR, Hoge GJ, Zigova T & Luskin MB (2002). Neural progenitor cells of the neonatal rat anterior subventricular zone express functional GABA(A) receptors. *J Neurobiol* **50**, 305–322.

Stewart RR, Zigova T & Luskin MB (1999). Potassium currents in precursor cells isolated from the anterior subventricular zone of the neonatal rat forebrain. *J Neurophysiol* **81**, 95–102.

Temple S & Alvarez-Buylla A (1999). Stem cells in the adult mammalian central nervous system. *Curr Opin Neurobiol* **9**, 135–141.

Verheugen JA, Fricker D & Miles R (1999). Noninvasive measurements of the membrane potential and GABAergic action in hippocampal interneurons. *J Neurosci* **19**, 2546–2555.

Verheugen JA, Vijverberg HP, Oortgiesen M & Cahalan MD (1995). Voltage-gated and Ca^{2+}-activated K^+ channels in intact human T lymphocytes. Noninvasive measurements of membrane currents, membrane potential, and intracellular calcium. *J Gen Physiol* **105**, 765–794.

Whiting PJ, Bonnert TP, Mckernan RM, Farrar S, Le Bourdelles B, Heavens RP, Smith DW, Hewson L, Rigby MR, Sirinathsinghji DJ, Thompson SA & Wafford KA (1999). Molecular and functional diversity of the expanding GABA-A receptor gene family. *Ann N Y Acad Sci* **868**, 645–653.

Wichterle H, Garcia-Verdugo JM & Alvarez-Buylla A (1997). Direct evidence for homotypic, glia-independent neuronal migration. *Neuron* **18**, 779–791.

Zigova T, Pencea V, Betarbet R, Wiegand SJ, Alexander C, Bakay RA & Luskin MB (1998). Neuronal progenitor cells of the neonatal subventricular zone differentiate and disperse following transplantation into the adult rat striatum. *Cell Transplant* **7**, 137–156.

Acknowledgements

This work was supported by supported by R21NS044161-01. We thank Dr C. A. Greer and Dr H. Treloar for helpful suggestions.